European Laboratory for Particle Physics

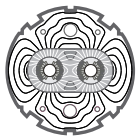

Large Hadron Collider Project

LHC Project Report 314

Coherent Beam-Beam Oscillations at the LHC.

M.P. Zorzano, F. Zimmermann, SL Division

Abstract

The transverse coherent motion of the two colliding LHC beams is studied by multi-particle tracking, where the beam-beam force is calculated assuming a Gaussian beam distribution with variable barycentres and rms beam sizes. The simulation yields the coherent and incoherent oscillation frequencies, the emittance growth of either beam, and evidence for the existence or lack of Landau damping. The transverse beam sizes change with the fractional part of the tune as expected from the dynamic beta effect. For head-on collisions, we find that the π-mode frequency lies outside of the continuum frequency spread if the ratio of the beam-beam parameters exceeds 0.6, in accordance with predictions [1]. For smaller ratios, the π-mode is Landau damped. When long range interactions are also included, undamped coherent modes do still exist outside the continuum, both with and without alternating crossing planes at two interaction points. However, the simulation shows that separating the tunes of the two beams can restore the Landau damping.

Administrative Secretariat
LHC Division
CERN
CH-1211 Geneva 23
Switzerland

Geneva, 2 November 1999

1 Introduction

Two colliding beams exert a force on each other which is focusing for opposite polarities and defocusing for equal polarity, as for the two proton beams at the LHC. It is predicted from the linearized Vlasov equation that, in the case of one bunch per beam with equal parameters (intensity, beam size, betatron tune), two dipole coherent modes of oscillation appear: the σ-mode whose frequency is equal to the unperturbed betatron tune, and the π-mode with a tune shift of 1.21 to 1.33 times the beam-beam parameter ξ [2]. The coefficient depends on the beam aspect ratio.

In addition to the coherent modes, there is a continuum spectrum due to the incoherent oscillations of individual particles in each beam. The incoherent tune shift ranges from 0 to ξ for particles at large and small betatron amplitudes. Generally one can expect Landau damping to occur for oscillation modes whose frequency lies inside this continuum band. The Landau damping is expected to be least effective for the π-mode since it is farthest from the continuum. The beam-beam interaction itself does not lead to instabilities unless the tune is near a resonance [3]. But the loss of Landau damping can result in an instability driven by any small impedance component of the vacuum chamber.

Moreover, the beam-beam interaction in the LHC is complicated by a non-zero crossing angle at the collision points and the large number of bunches. This leads to about 30 long range beam-beam collisions in each interaction region, where the two beams are not fully separated into different vacuum chambers. These parasitic collisions can also give rise to coherent modes and create additional tune shifts.

At the LHC-99 beam-beam workshop held at CERN [4], concern was raised regarding the stability of colliding beams with large and equal incoherent tune shifts. It has been predicted that the frequency of the π-mode moves out of the continuum for a ratio of beam-beam parameters $r > 0.6$ [1]. At the same workshop it was suggested as a potential cure to decouple the two beams by making their tunes unequal [5, 6]. So far there have been no theoretical predictions of the coherent modes in the presence of parasitic collisions. These open questions motivated our tracking studies.

In this report, we investigate the frequency spectrum of the centroid bunch motion using a multiparticle tracking code written in C. The simulation model is described in Section 2. Section 3 presents results for head-on collisions of bunches with equal tunes, considering both round and flat beams. Here, we compare the obtained tune shifts of the coherent modes with those predicted by the linearized Vlasov theory, and, for round beams, we determine the tune shift of the coherent dipole modes and its consequences on Landau damping and emittance growth as a function of the beam-beam parameter ratio. The dependence on the nominal betatron tune is explored in Section 4. In Section 5, we describe simulation results including long range collisions, with and without alternating crossing planes. Finally, in Section 6 we consider the collision of two beams with unequal tunes, where the coherent dipole modes disappear.

2 The model

We simulate the collision of two strong proton beams. Our system of normalized variables is $x = \frac{X}{\sigma_{oX}}$, $v_x = \frac{\beta X'}{\sigma_{oX}}$, $y = \frac{Y}{\sigma_{oY}}$, $v_y = \frac{\beta Y'}{\sigma_{oY}}$ where $\sigma_{oX} = \sigma_{oY} = \sigma$ are the nominal horizontal and vertical rms sizes, and β the betatron function. The prime denotes the derivative with respect to longitudinal position s, so that *e.g.*, X' is the horizontal trajectory slope.

We represent each of the beams by a set of N macroparticles, whose motion is followed over n turns, assuming linear betatron motion and a strong beam-beam collision

at one interaction point (IP). At this IP, each particle in the bunch experiences a deflection from the field of a counter rotating Gaussian beam with barycentres at $(\bar{x}^{(i)}, \bar{y}^{(i)})$ and squared transverse sizes $M_{xx}^{(i)} =< (x^{(i)} - \bar{x}^{(i)})^2 >$, $M_{yy}^{(i)} =< (y^{(i)} - \bar{y}^{(i)})^2 >$. If $M_{xx}^{(i)} > M_{yy}^{(i)}$ the horizontal beam-beam kick is

$$\Delta v_x(n) = \frac{r_p N_p^{(i)}}{\gamma} \frac{\beta}{\sigma^2} F_x(x - \bar{x}^{(i)}, y - \bar{y}^{(i)}, M_{xx}^{(i)}, M_{yy}^{(i)}) \tag{1}$$

with

$$\begin{aligned} F_x(x, y, M_{xx}, M_{yy}) &= \sqrt{\frac{2\pi}{(M_{xx} - M_{yy})}} \Im \left[W\left(\frac{x + iy}{\sqrt{2(M_{xx} - M_{yy})}} \right) \right. \\ &- \left. \sqrt{\frac{2\pi}{(M_{xx} - M_{yy})}} e^{(-\frac{x^2}{2M_{xx}} - \frac{y^2}{2M_{yy}})} W\left(\frac{x\sqrt{M_{yy}/M_{xx}} + iy\sqrt{M_{xx}/M_{yy}}}{\sqrt{2(M_{xx} - M_{yy})}} \right) \right], \end{aligned} \tag{2}$$

where W denotes the complex error function [7] (if $M_{yy}^{(i)} > M_{xx}^{(i)}$ substitute x by y on both sides of the equation, and vice versa). The vertical beam-beam force is described by the real part of the same expression. In these maps the superindex (i) indicates variables of the counter-rotating beam.

The linear map from one IP to the next is

$$\begin{pmatrix} x(n+1) \\ v_x(n+1) \end{pmatrix} = \begin{pmatrix} \cos(2\pi Q_x) & \sin(2\pi Q_x) \\ -\sin(2\pi Q_x) & \cos(2\pi Q_x) \end{pmatrix} \begin{pmatrix} x(n) \\ v_x(n) + \Delta v_x(n) \end{pmatrix} \tag{3}$$

An equivalent map is applied in the vertical plane, (y, v_y).

In the simulation, the initial coordinates (x, v_x, y, v_y) for two groups of N macroparticles representing either of the two beams are selected from a Gaussian random distribution in each variable with $< x >=< v_x >=< y >=< v_y >= 0$ and $< x^2 >=< v_x^2 >=< y^2 >=< v_y^2 >= 1$.

Note that a multiparticle tracking model like this was used by E. Keil for the study of 2 dimensional flat beams [8] and later by S. Matsumoto and K. Hirata [9], who found good agreement between simulation results and analytical predictions for the vertical motion of flat beams.

Typical parameters used in the simulation are fractional betatron tunes of $Q = Q_x \approx Q_y = 0.32$, the number of protons in beam 1 $N_p^{(1)} = 1.05 \times 10^{11}$, the number of protons in the 2nd beam $N_p^{(2)} = r \times N_p^{(1)}$, where r lies within $(0, 1)$, $\gamma = E/E_0$ with $E = 7$ TeV, r_p the classical radius of the proton, horizontal and vertical rms beam sizes of $\sigma = 16 \cdot 10^{-6}$ m and a beta function $\beta_{x,y} = 0.5$ m. These values define the so-called beam-beam parameters in the two transverse planes via

$$\xi_{x,y}^{(i)} = \frac{N_p^{(i)} r_p \beta x, y}{2\pi\gamma\sigma_{x,y}(\sigma_x + \sigma_y)} \tag{4}$$

with $i = 1$ for beam 1, and $i = 2$ for beam 2. The ratio of the beam-beam parameters, $r = \xi^{(2)}/\xi^{(1)}$, determines the behaviour of the system [1]. For $r = 0$ we have the weak-strong limit, and for $r = 1$ the strong-strong limit.

In the case of nearly equal horizontal and vertical squared beam sizes, $M_{xx}^{(i)} \approx M_{yy}^{(i)}$, the expression of Eq. (2) is ill defined. We then use a simpler expression for the force:

$$F_x(x, y, M_{xx}^{(i)}, M_{yy}^{(i)}) = \frac{2x}{(x^2+y^2)} \left[1 - \exp\left(-\frac{x^2+y^2}{M_{xx}^{(i)} + M_{yy}^{(i)}}\right)\right]. \tag{5}$$

In order to speed up the calculation, we have also performed a series of simulations using only this simplified expression. The results for (initially) round beams and equal transverse tunes are qualitatively and quantitatively the same as obtained using the exact expression of the force, Eq. (2). This seems to indicate that small variations in the relative transverse beam sizes do not affect much the properties of the coherent modes.

For the simulation of parasitic (long range) collisions, the same model is employed, assuming round beams. The two beams collide with a horizontal separation L_x (in units of σ_x). There is about 90° phase advance between the IP and the long range collision region. Since the betatron phase advance between the long range collisions on one side of the interaction region is very small, we lump all n_{par} parasitic collisions into a single one, to reduce the computing time. This overestimates the effect slightly because the bunches oscillate with different phases with respect to each other [10]. Because a static dipole kick would change the closed orbit of the bunch, the static kick from the long range collision must be subtracted. The beam-beam long range kick used in our simulation code is then

$$\begin{aligned} \Delta v_x(n) = \; &+ \; n_{par} \frac{2 r_p N_p^{(i)}}{\gamma} \frac{\beta}{\sigma^2} \left\{ \frac{(x - \overline{x}^{(i)} - L_x)}{R^2} \left[1 - \exp\left(-\frac{R^2}{M_{xx}^{(i)} + M_{yy}^{(i)}}\right)\right]\right\} \\ &- \; n_{par} \frac{2 r_p N_p^{(i)}}{\gamma} \frac{\beta}{\sigma^2} \left\{ \frac{(-L_x)}{\hat{R}^2} \left[1 - \exp\left(-\frac{\hat{R}^2}{M_{xx}^{(i)} + M_{yy}^{(i)}}\right)\right]\right\} \end{aligned} \tag{6}$$

where

$$R^2 = (x - \overline{x}^{(i)} - L_x)^2 + (y - \overline{y}^{(i)})^2 \tag{7}$$

$$\hat{R}^2 = (L_x)^2 + (y - \overline{y}^{(i)})^2. \tag{8}$$

At the LHC, there are about $n_{par} = 16$ parasitic encounters on each side of an IP, with a minimum transverse separation of $L_x = 7.5$ (in units of σ_x).

3 Head-on collision with equal betatron tunes

3.1 π- and σ-modes for round beams

First let us consider the strong-strong case, $r = 1$, and head-on collisions of two bunches, using the maps (1)+(3) with the beam-beam force $F(x, y)$ of Eq. (2). The statistical variation in the distribution of particles is sufficiently large to excite the coherent modes. The transverse squared beam sizes, M_{xx} and M_{yy}, oscillate around 1 (in units of σ^2) with a maximum deviation of 2 %. Thus the beam stays approximately round.

If we Fourier analyse the motion of the barycentre of one bunch, we find two coupling modes. One is located at Q, the other has a lower frequency. In Fig. 1 we plot the amplitude frequency spectrum on a logarithmic scale. The horizontal axis gives the tune shift from the unperturbed tune Q in units of ξ (namely: $w = \frac{\nu - Q}{\xi}$; for the round beam case $\xi_x = \xi_y = \xi = 0.003355$, $Q = 0.32$). For the other beam a similar picture is obtained. Fourier analysing the distance between the centroids ($< x^{(1)} > - < x^{(2)} >$,$< y^{(1)} > - < y^{(2)} >$)

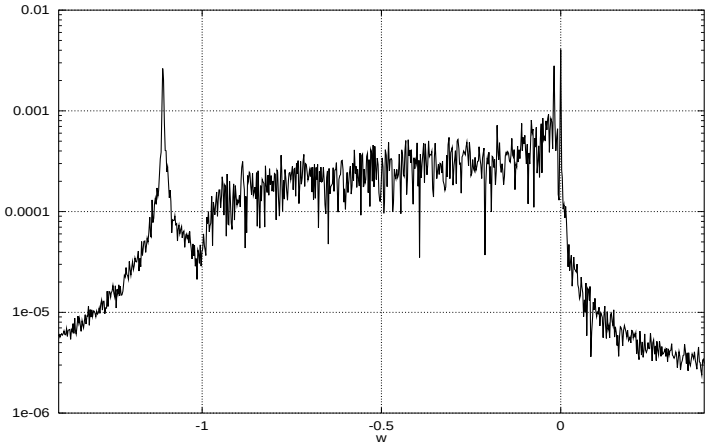

Figure 1: Frequency spectrum of the bunch centroid motion (over 2^{17} turns, $N = 10^4$ macroparticles) for round beams. The horizontal axis gives the tune shift from the unperturbed tune Q in units of ξ, *i.e.* $w = \frac{\nu - Q}{\xi}$. The vertical axis is the corresponding amplitude in logarithmic scale. The π- and σ- oscillation modes are clearly visible.

the coherent mode at the unperturbed frequency disappears. On the other hand, when we Fourier analyse the sum of the centroids ($< x^{(1)} > + < x^{(2)} >$,$< y^{(1)} > + < y^{(2)} >$) the lower mode frequency disappears. We can thus identify the mode at the unperturbed frequency as the so-called σ-mode, for which the centroids of the bunches oscillate in phase with equal frequencies and amplitudes. The lower frequency mode is called π-mode. In this mode the centroids oscillate also with equal frequencies and amplitudes but in opposite phase. The motion of the bunch centroids is a superposition of these two modes.

Between the π- and the σ-mode in Fig. 1 we can also see the *continuum*. This arises as follows. A single particle of beam 1 crossing beam 2 at a distance from its axis feels a focusing force which leads to a change in its tune. For particles near the centre of the counter rotating beam this tune shift is equal to $-\xi$. For particles further away the focusing force is smaller (due to the non-linearity of the beam-beam force). This creates an incoherent tune spread which extends from 0 to $-\xi$.

In our simulations we find the π-mode at a tune shift of -1.1 in units of ξ (and $\xi = 0.003355$). The π-mode is thus shifted outside of the continuum. Theoretical studies based on the Vlasov equation predict a tune shift between these σ- and π-modes equal to $Y \times \xi$, with Y the so-called Yokoya factor [2]. For the case where the two beams are round we expect $Y = 1.21$. This factor describes the change of the observable tunes caused by the distortion of the beam distribution due to the beam-beam collision. The tune shift is derived by means of a linearized Vlasov equation, assuming the unperturbed solution to be Gaussian. The shift obtained in our simulations is smaller than the theoretical prediction. The difference is either due to the simplifying assumptions of our model, where the beam-beam forces are calculated assuming that the beams are of Gaussian shape, or it is caused by approximations in the theoretical derivation [1)].

[1)] The beam-beam interaction can also excite coherent higher-order multipole modes in phase space. For the quadrupole mode a tune shift of $\Delta_\pi = -2 \times 1.022 \times \xi$ is predicted. The frequencies of the higher modes are much closer to the continuum. These modes may thus experience residual Landau damping. This could explain why, in the simulation, we have not observed any coherent quadrupole oscillations. Note that the quadrupole-mode continuum ranges from $2Q$ to $2Q - 2\xi$.

To illustrate the dynamics of the two beams we track $N = 10^5$ macroparticles for 2^{17} turns using a one dimensional model (with $F_x = \frac{2}{(x-\overline{x}^{(i)})}[1-\exp(-(x-\overline{x}^{(i)})^2/2M_{xx}^{(i)})]$). We group the macroparticles in histograms to get the density $\rho(x,t)$. To excite the coherent modes strongly we give an offset to one of the beams of 0.4 (in units of σ). Fig. 2-(top-left) illustrates the initial Gaussian distribution of the two beams, while the other three figures depict the distribution for the last three turns. Comparing the left lower picture in Fig. 2 with the initial distribution, on top, reveals that the distribution of the oscillating beam deviates from a Gaussian, the core participating more strongly in the oscillation.

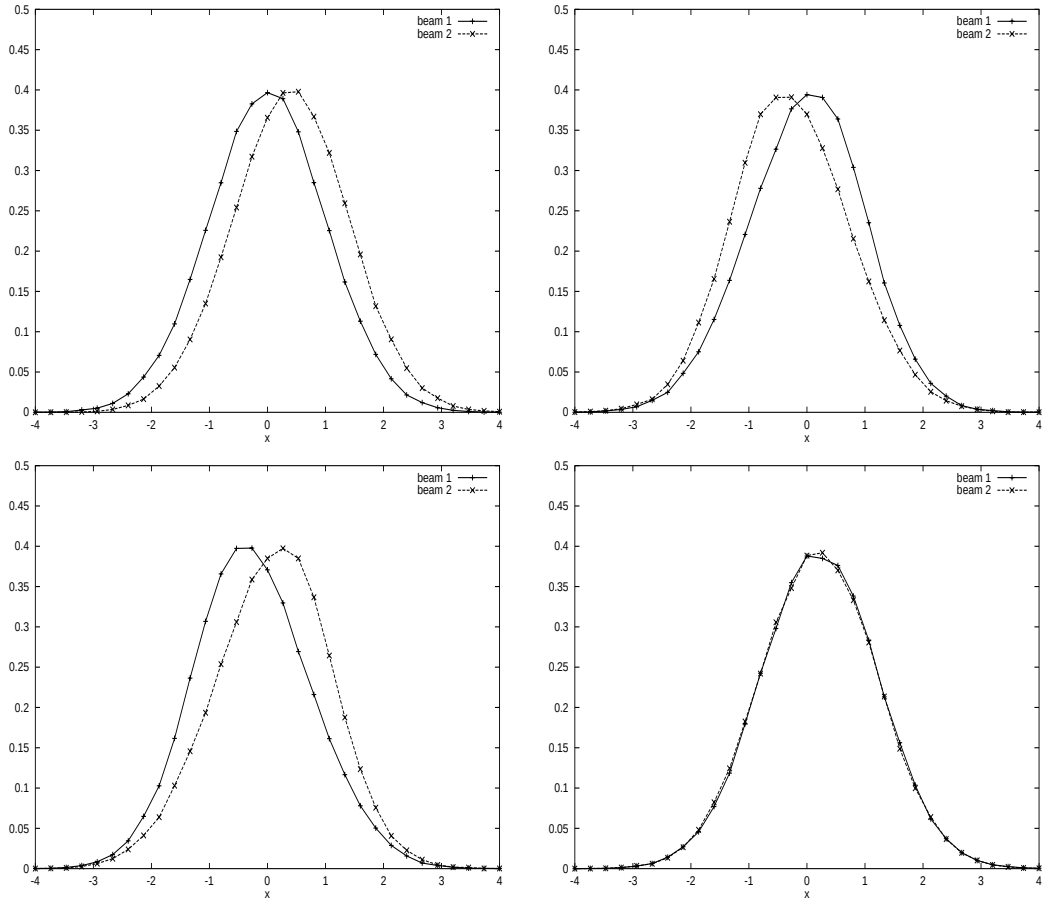

Figure 2: Dynamics of the two strong beams ($N = 10^5$ macroparticles, $Q = 0.32$) in a one dimensional simulation for round beams. Top-left: initial state. Top-right: after $2^{17} - 2$ turns, bottom-left: after $2^{17} - 1$ turns, bottom-right: after 2^{17} turns. The core of the beam oscillates coherently and the tails do not move.

3.2 π- and σ-modes for flat beams

The tune shift of the coherent π-mode depends on the vertical-to-horizontal aspect ratio at the collision point. We have simulated the collision of two flat beams with $\sigma_x = 16 \times \sigma_y$ (which is a rather typical parameter for e^+/e^- storage rings) and $N_b = 1.01 \times 10^{13}$ (we artificially increase the number of particles per bunch in order to keep ξ big and have a big frequency spread). In this case we find a vertical coherent π-mode with a tune shift of $-1.09 \times \xi_y$ ($\xi_y = 0.03691$), and a horizontal tune shift of $-1.15 \times \xi_x$ ($\xi_x = 0.002466$). In the case of very flat beams the linearized Vlasov theory predicts a tune shift of $-1.24 \times \xi_y$

for the vertical π-mode and of $-1.33 \times \xi_x$ for the horizontal π-mode. In Fig. 3 we show the spectrum of the centroid motion of one of the two beams. The horizontal axis is the distance to the unperturbed tune in units of the corresponding beam-beam parameter [2)].

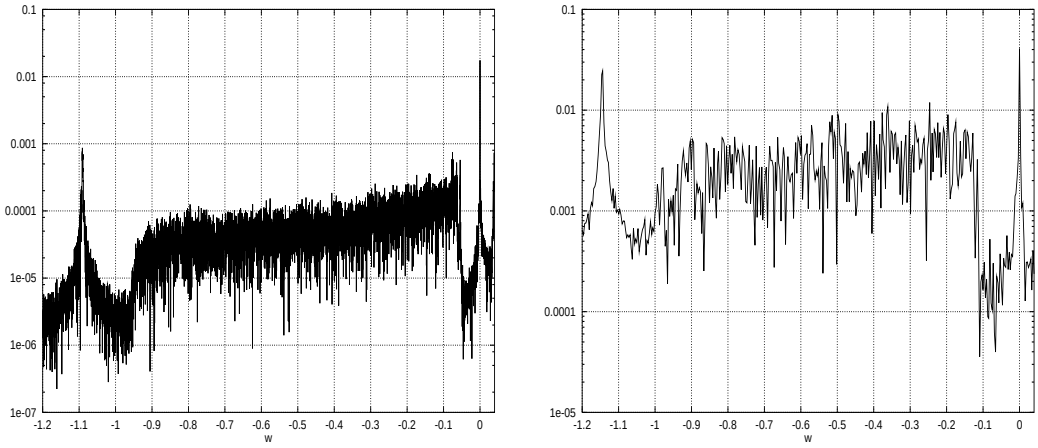

Figure 3: Frequency spectrum of the vertical (left) and horizontal (right) bunch centroid motion for flat beams (over 2^{17} turns, $N = 10^4$ macroparticles). The tune shift of the π-mode with respect to the σ-mode is different for each plane.

3.3 Landau damping

The case of interest for proton machines is the round beam limit and we will concentrate on this case from now on.

In the σ-mode the beams oscillate in phase at the IP without changing their shape. Participating in the π-mode are mainly particles with small betatron amplitudes, which are most strongly affected by the movements of the opposing beam. This explains the large value of the coherent tune shift [1, 2]. In the weak-strong case $r \to 0$ such a mode does not exist (unlike the discrete σ-mode which exists at any value of the intensity ratio). Therefore, if one reduces the intensity of one of the beams there must be a point where the discrete π-mode disappears. If the frequency of the π-mode lies within the incoherent tune spread its energy can be absorbed by individual particles with similar oscillation frequencies. This phenomenon is known as Landau damping [12]. As a consequence the π-mode will disappear and the emittance will grow until the π-mode energy has been completely absorbed.

Next we study the system for different values of the parameter r. We give an initial horizontal offset $d = +0.2$ (in units of σ_x) to the distribution of one beam. This excites the coherent dipole modes. The frequency spectrum for an intensity ratio $r = 1$ is depicted in Fig. 4, where the amplitudes of both σ- and π-mode are plotted (calculated from the sum and from the difference of the two beam centroids). The figure shows that the π-mode is outside the continuum and not damped. The case $r = 0.6$ is illustrated in Fig. 5, comparing the π-mode at two consecutive time intervals of 2^{16} turns, demonstrating that the amplitude of the π-mode decreases in time. Thus, for $r = 0.6$, we find that the π-mode frequency lies near the edge of the continuum, and is marginally Landau damped. For the

[2)] Similar calculations were presented in reference [11] for the collision of e^+/e^- following the evolution of 500 macroparticles over 500 turns and obtaining, for a simulation with $Q_x = 0.25$, $Q_y = 0.3$ and $\xi_y = 0.0306$, a vertical tune shift of the π-mode of $1.06 \times \xi_y$.

case $r = 0.3$ (not shown), the π-mode is well inside the continuum, and it is damped rapidly. This is in agreement with the prediction of Y. Alexahin stating that in the cases where the ratio $r \leq 0.6$ the π-mode frequency lies within the incoherent tune spread of the weaker beam [1].

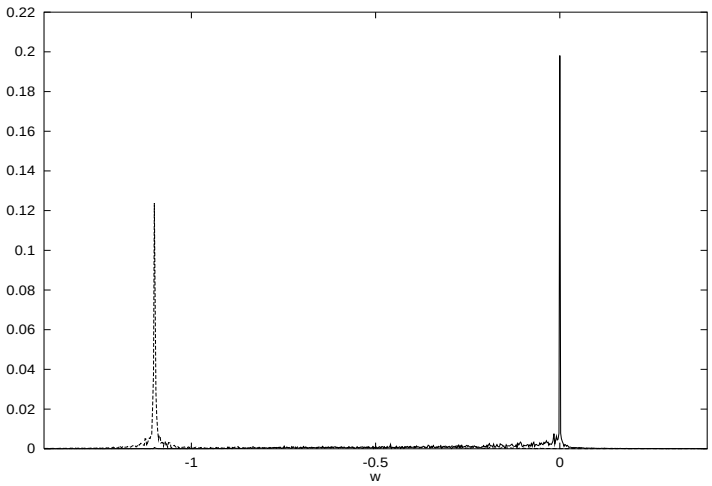

Figure 4: Frequency spectrum of the centroid motion (over 2^{17} turns, $N = 10^4$) for the case of round beams colliding head-on with an initial offset of $d = 0.2$ (in units of σ_x). The ratio of beam-beam parameters is equal to $r = 1$. The horizontal axis gives the tune shift from the unperturbed tune Q in units of ξ, *i.e.* $w = \frac{\nu - Q}{\xi}$. The vertical axis is the corresponding amplitude. The π-mode at -1.1 has not been damped and its amplitude is constant over this time.

3.4 Emittance growth

The energy of the kick is distributed among different oscillation modes: a coherent σ-mode, a coherent π-mode and an incoherent spectrum of oscillations. The fraction of energy which is imparted on the continuum leads to an irreversible emittance growth. We study, for different values of r, the emittance growth and energy distribution for the case of round beams with emittances $\epsilon_x = \epsilon_y$, and after a horizontal kick of magnitude $d = 0.2$ (in units of σ_x).

Let us express the horizontal and vertical oscillation energy in terms of a generalised 'emittance', defined as

$$\begin{aligned} \epsilon_x &= < x^2 + v_x^2 > \\ \epsilon_y &= < y^2 + v_y^2 >, \end{aligned} \tag{9}$$

where the angular brackets denote an average over the bunch distribution. In order to measure the irreversible emittance growth, we subtract the centroid motion [3)]

$$\begin{aligned} \epsilon_x^I &=< (x - \overline{x})^2 + (v_x - \overline{v}_x)^2 > \\ \epsilon_y^I &=< (y - \overline{y})^2 + (v_y - \overline{v}_y)^2 > . \end{aligned} \tag{10}$$

[3)] If there is no average correlation between position and velocity (*i.e.*, $< x v_x >= 0$ and $< y v_y >= 0$), and if the dynamic beta beat is small, this definition agrees with the usual definition of emittance $\epsilon_x = (< (x - \bar{x})^2 >< (v_x - \bar{v}_x)^2 > - < x v_x >^2)^{1/2}$ except for a factor of two.

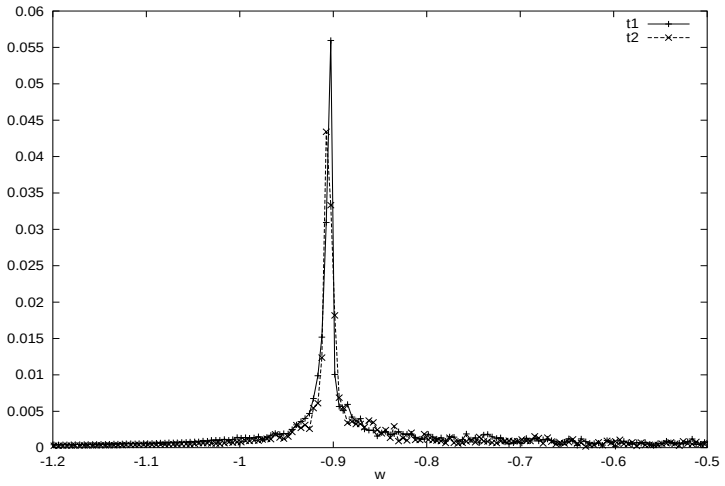

Figure 5: Frequency spectrum of the centroid motion at two successive time intervals of 2^{16} turns ($N = 10^4$), considering head-on collisions of two round bunches with beam-beam parameter ratio $r = 0.6$ and initial offset of $d = 0.2$ (in units of σ_x). The π-mode at -0.9 is Landau damped. Solid line and plus symbols: first time interval; dashed line and crosses: second interval.

It is shown in Fig. 4 that, for $r = 1$, the energy is distributed among a σ-oscillation mode of amplitude $A = 0.2$, a π-mode of approximate amplitude $B \approx 0.13$ (notice the broad base of the π-mode peak) and the continuum. The fraction of energy absorbed by the continuum leads to an irreversible emittance growth $\Delta\epsilon^I = (\epsilon_x^{(1),I} + \epsilon_y^{(1),I})/\epsilon_0 - (\epsilon_x^{(2),I} + \epsilon_y^{(2),I})/\epsilon_0 - 2$ of $\Delta\epsilon^I \approx 0.004$; see the lower curve in Fig. 6.

For $r \leq 0.6$ the frequency of the π-mode lies in the continuum and is Landau damped. The emittance grows until this mode has completely been absorbed. Examples are the two upper curves in Fig. 6. In this case, the final emittance growth is larger: $\Delta\epsilon^I \approx 0.01$.

The beam response to a kick has also been studied, for the case $r = 1$, using the Vlasov equation [1]. After a horizontal kick of magnitude d (in units of σ_x) the horizontal emittances of the perturbed beams are predicted to be [1]:

$$\frac{\epsilon_x^{(1)}}{\epsilon_0} + \frac{\epsilon_x^{(2)}}{\epsilon_0} = 2 + \frac{d^2}{2}(0.5 + 0.32 + 0.18) \tag{11}$$

The first term in the brackets describes the fraction of energy carried by the σ-mode, the second represents the energy of the π-mode, and the last is the fraction which is imparted on the continuum leading to an irreversible emittance growth. In our two dimensional model, this energy is distributed between the two planes. Therefore we expect a total emittance

$$\frac{\epsilon_x^{(1)} + \epsilon_y^{(1)}}{\epsilon_0} + \frac{\epsilon_x^{(2)} + \epsilon_y^{(2)}}{\epsilon_0} = 2 + \frac{d^2}{2}(0.5 + 0.32 + 0.18) \tag{12}$$

where $\epsilon_0 = (\epsilon_x + \epsilon_y) = 4$. The σ-mode of centroid oscillation, with amplitude A, carries an energy $A^2 = \epsilon_0 \times \frac{d^2}{2} \times 0.5$. The π-mode with amplitude B has an energy $B^2 = \epsilon_0 \times \frac{d^2}{2} \times 0.32$ and the relative irreversible growth of emittance is $\Delta\epsilon^I = \frac{d^2}{2} \times 0.18$. For $d = 0.2$ then $A = 0.2$, $B = 0.16$ and $\Delta\epsilon^I = 0.0036$. This is in very good agreement with the amplitudes shown in Fig. 4 and with the emittance growth shown in the lower curve of Fig. 6.

For the case where $r \leq 0.6$ the energy of the π-mode is transfered to the continuum. The expected emittance growth is then $\Delta\epsilon^I = \frac{d^2}{2} \times (0.18 + 0.32) = 0.01$, which is also in agreement with the results shown in Fig. 6.

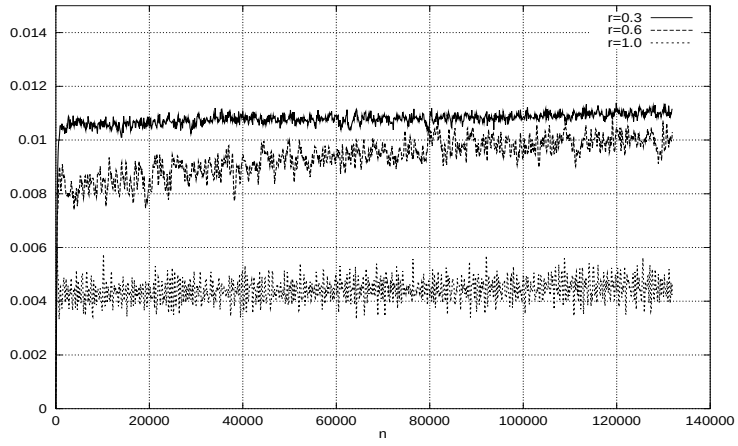

Figure 6: Irreversible emittance growth $\Delta\epsilon^I$ (vertical axis) as a function of time (horizontal axis, time in turns) for three different ratios of beam-beam parameters, $r = 0.3$, $r = 0.6$ and $r = 1$. The beams are perturbed by an initial offset of $d = 0.2$ (in units of σ). If $r \leq 0.6$ the frequency of the π-mode lies in the continuum and the mode is Landau damped. The emittance will grow until all its energy has been absorbed. For $r = 1$ the π-mode is not Landau damped, and carries part of the energy of the kick. The emittance growth is then smaller.

4 Tune shift dependence on the working point

For the LHC, three working points are proposed where the calculated tune footprint can be lodged: point 1 ($Q_x = 0.31$, $Q_y = 0.32$), point 2 ($Q_x = 0.23$, $Q_y = 0.24$) and point 3 ($Q_x = 0.38$, $Q_y = 0.39$) [13]. In all these points there is a difference of order 0.01 between the vertical and horizontal tune. We will first ignore this in our calculations and track only the dependence on the working point tune with $Q_x = Q_y$. Later we will present results for separated tunes.

4.1 Dynamic beta effect

Tab. 1 lists the tune shift between the coherent π-mode and the σ-mode in units of ξ_0 for different nominal tunes, obtained by tracking over 2^{17} turns with an initial beam-beam parameter of $\xi_0 = 0.003355$. In all cases, the continuum extended from 0 to roughly ξ_0, with the π-mode outside of it. Since we observed that the transverse size decreases as the fractional part of the tune approaches the half integer and increases when it gets closer to the integer from above, we include in the table the ratio of the average (over 2^{17} turns) measured beam size to the initial value $(\overline{M}_{xx} + \overline{M}_{yy})/2 = \sigma^2/\sigma_0^2$.

We attribute the variation in the beam size with tune to the dynamic beta effect, which is the simplest phenomenon in the strong-strong picture including static distortions. This effect can be analysed by modelling the beam-beam interaction as a linear defocusing lens which alters the β seen by the particle [14]. Assuming a linearized beam-beam force the perturbed steady-state remains Gaussian, and only the rms beam size changes. In a linear approximation the map experienced by a particle near the centre of the counter-rotating beam is

Q	Δ_π/ξ_0	σ^2/σ_0^2
0.01	-1.135	1.1887
0.05	-1.112	1.0335
0.10	-1.11	1.0148
0.24	-1.108	1.0007
0.32	-1.108	0.9952
0.39	-1.108	0.9874
0.49	-1.102	0.8581

Table 1: Tune split between the π- and σ-mode in units of ξ_0 and ratio of the beam size to the initial value $\sigma^2/\sigma_0^2 = (\overline{M}_{xx} + \overline{M}_{yy})/2$ for different nominal tunes.

$$\begin{pmatrix} \cos(2\pi Q) & \beta\sin(2\pi Q) \\ -\frac{1}{\beta}\sin(2\pi Q) & \cos(2\pi Q) \end{pmatrix} \begin{pmatrix} 1 & 0 \\ -\frac{4\pi\xi}{\beta} & 1 \end{pmatrix} = \begin{pmatrix} \cos(2\pi\hat{Q}) & \hat{\beta}\sin(2\pi\hat{Q}) \\ -\frac{1}{\hat{\beta}}\sin(2\pi\hat{Q}) & \cos(2\pi\hat{Q}) \end{pmatrix}, \quad (13)$$

where ξ includes the perturbed sizes of the counter-rotating beam: $\xi = N_p r_p \beta/(4\pi\gamma\sigma^2) = \xi_0\sigma_0^2/\sigma^2$. Notice that the perturbed sizes scale with the perturbed beta-functions as $\sigma^2/\sigma_0^2 = \hat{\beta}/\beta$, since we assume that the beam emittances are unchanged by the beam-beam interaction. The new beta function, $\hat{\beta}$, and the equilibrium rms beam size, can be found self-consistently as a function of the unperturbed parameters [14]:

$$\frac{\beta}{\hat{\beta}} = \sqrt{1 - \left(\frac{2\pi\xi_0}{\sin(2\pi Q)}\right)^2} - 2\pi\xi_0\cot(2\pi Q). \quad (14)$$

Integrating the beam-beam force over the Gaussian distribution, the effective beam-beam force is one half that experienced by a single particle near the beam centre [15]. We evaluate then the dynamic beta effect replacing in Eq. (14) ξ_0 by $\Xi = \xi_0/2$.

In Fig. 7 we plot the size-ratio σ^2/σ_0^2 of Tab. 1 (points) obtained from tracking and the theoretical prediction (line). The agreement is excellent. Note that when the fractional part of the tune approaches the half integer from below, β and the rms beam size σ decrease, an effect which has been experimentally observed in e^-/e^+ collisions at CESR [16]. For machines such as LEP with a large beam-beam parameter this effect has a strong influence on the optics and beam-dynamics [17].

Regardless of the dynamic beta effect, the tune shift of the π-mode appears to decrease as the fractional part of the tune increases.

4.2 Different vertical and horizontal tune

Next we track for different vertical and horizontal tune. We keep Q_x constant at 0.31 and vary Q_y. We do not find any special resonance effect when Q_x and Q_y approach each other[4)]. The reduction of the vertical size for increasing fractional tune is again consistent with the dynamic beta effect; see Tab. 2.

[4)] In the case of flat beams, and scanning for different vertical tunes, it was found in [11] that the vertical size increases very strongly when $(Q_x \pm Q_y)\text{mod k} \approx 0$ and when $2Q_y\text{mod k} \approx 0$. The first of these resonances may be explained by an exchange of horizontal and vertical emittances, *i.e.* coupling.

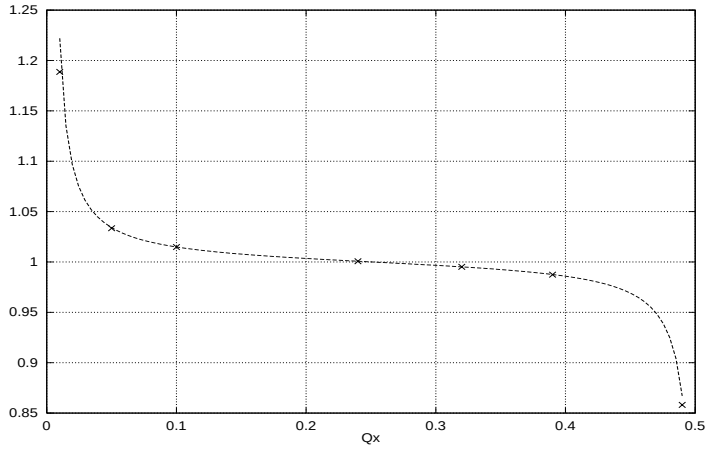

Figure 7: Comparison of the tracking results with the theoretical dynamic beta effect. Vertical axis: beam size ratio σ^2/σ_0^2, horizontal axis fractional tune. Points: data of Table 1 obtained from tracking; curve: $\sigma^2/\sigma_0^2 = \hat{\beta}/\beta$ dynamic beta theoretical prediction according to Eq. (14). When the fractional part of the tune approaches the half integer from below, β and the rms beam size σ decrease.

Q_y	Δ_{π_y}/ξ_0	$\overline{M}_{yy}/1.0$
0.24	-1.104	1.0010
0.28	-1.103	0.9982
0.30	-1.102	0.9971
0.32	-1.101	0.9950
0.34	-1.1	0.9934
0.36	-1.099	0.9916
0.39	-1.098	0.9877

Table 2: Tune split between the vertical π- and σ-mode in units of ξ_0 and ratio of the beam vertical size to the initial value for different vertical tunes and $Q_x = 0.31$.

5 Long range collisions with equal-tunes

We have repeated the calculations of Section 3.1, where the beam stayed nearly round, using the approximate formula (5). We obtained the same results with much shorter computing time. From now on, we will employ this simplified formula to reduce the CPU time. We choose equal vertical and horizontal tune ($Q_x = Q_y = 0.32$).

5.1 Horizontal crossing (no head-on collisions)

Since the transverse distance between two bunches in the long range collision is larger than the rms beam size, the effects will be similar to the coherent interaction of rigid point like bunches. The contribution of parasitic crossings to the tune shift of coherent oscillation modes is then expected to be

$$\Delta\nu_\pi = 2 \times (\text{incoherent tune shift}) \quad (15)$$

$$\Delta\nu_\sigma = 0. \quad (16)$$

Moreover the incoherent tune shift for beam separations larger than $\approx 1.5\ \sigma$ has different signs for the two planes.

Fig. 8 shows the horizontal and vertical spectrum of centroid oscillation of one bunch subject to long range collisions with a horizontal separation of $L_x = 7.5$ (in units of σ_x). The horizontal axis gives the tune shift from the unperturbed tune Q in units of ξ: $w = \frac{\nu - Q}{\xi}$. In the horizontal plane, the incoherent spectrum has positive tune shifts, and the coherent dipole π-mode is visible at twice the incoherent tune shift. In the vertical plane, the incoherent spectrum has negative tune shifts and again the coherent π-mode is shifted twice as much.

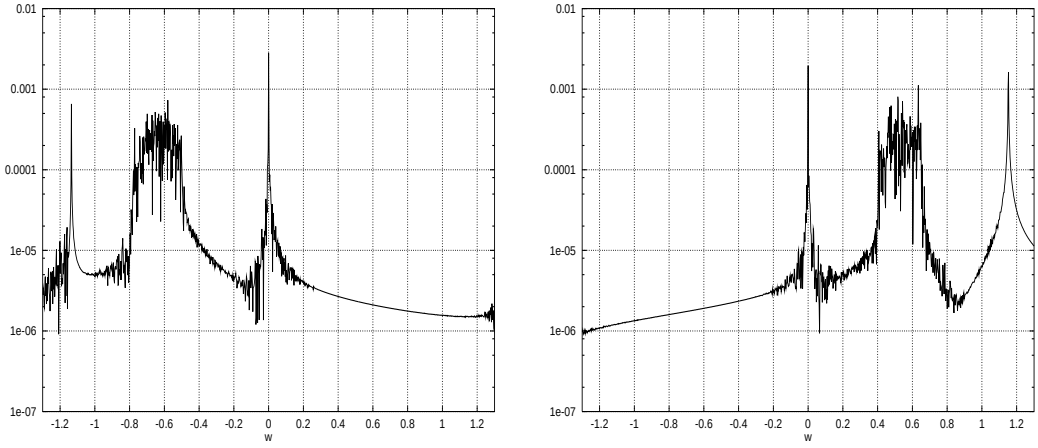

Figure 8: Spectrum of the vertical (left) and horizontal (right) centroid motion for long range collision with horizontal separation $L_x = 7.5$ (in units of σ_x) and no head-on collision (2^{17} turns, $N = 10^3$ macroparticles). The tune shift due to long range collisions has opposite sign in the two transverse planes. The coherent π-mode is at twice the incoherent tune shift.

5.2 Head-on collisions and horizontal crossing

Next we study the combined effect of head-on and long range interactions. We consider two closely spaced bunches per beam, and two interaction regions. We denote the bunches in beam 1 as a and b, and those in beam 2 as c and d. First two bunches collide head-on (for instance a-c). We then apply a phase advance of 90° to reach the long range collision region. There the bunch pairs (a-d) and (b-c) are collided with a horizontal separation of L_x and a beam-beam parameter n_{par} times stronger than for the single-bunch long range collision to take into account the additive effect of n_{par} parasitic collisions. Subsequently, we advance the phase of the beams to reach the other interaction region, where now bunches b and d are collided head-on (b-d). This is followed by another phase advance of 90° to the long range collision point, where again long range collisions of the pairs (a-d) and (b-c) are applied. In this new collision scheme the two bunches of each beam are coupled with both bunches in the opposing beam. Therefore, we expect to find 4 coherent modes in each plane. Note that in this scheme each bunch only performs half of the head-on collisions (one, instead of the two corresponding to the two IPs) and half of the parasitic crossings (we only consider n_{par} long range collisions *after* the IP), to save computing time and reduce the complexity (later on we will consider a case where each bunch has two head-on collisions and double number of long range interactions).

Fig. 9 shows the spectrum of amplitudes of one bunch, in the vertical (left) and horizontal (right) plane. Clearly visible are the lines of the 4 coherent modes. Three of these are outside of the continuum.

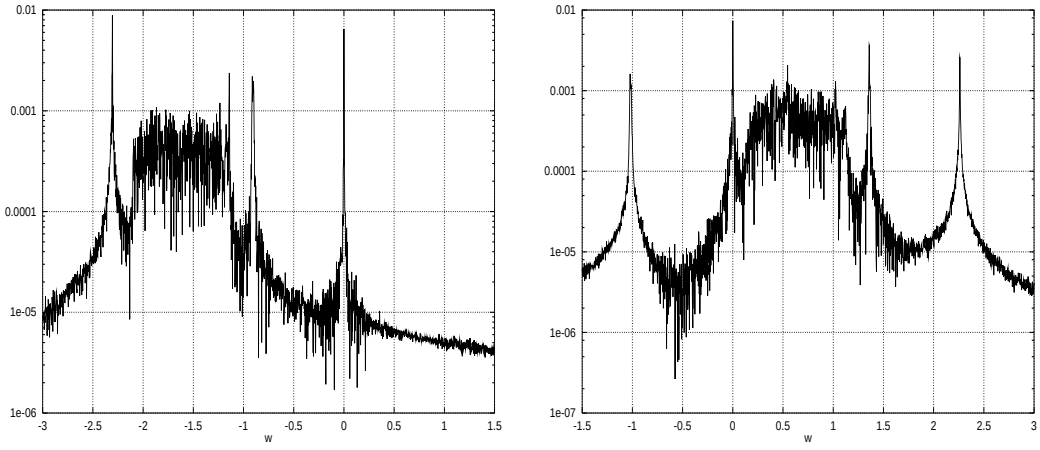

Figure 9: Spectrum of the vertical (left) and horizontal (right) motion of a bunch centroid (2^{17} turns, $N = 10^3$macroparticles) for the case of head-on collision and horizontal crossing with separation $L_x = 7.5$ (in units of σ). The two bunches of one beam are coupled with the two bunches in the opposing beam and thus we find 4 coherent modes in each plane.

5.3 Head-on collisions with alternating crossing

Since the tune shifts from long range collisions have opposite signs in the two transverse planes, for the LHC an alternating crossing scheme was proposed [18], where the beams are separated in orthogonal planes at the two main IPs. This reduces the overall incoherent tune shift and tune spread by compensation between the IPs. As a consequence, the frequency shifts of the coherent modes are reduced.

We collide the 2×2 bunches as before, except that in the second long range interaction region the bunches collide vertically with the separation $L_y = 7.5$ (in units of σ_y). Now the two planes of oscillation are equivalent and the coherent modes are shifted closer to the continuum. In the case of collisions of equally strong beams, we again find 3 coherent modes outside the continuum, as illustrated in Fig. 10. The figure on the left shows the result obtained with the round beam approximation, for comparison, the figure on the right shows the one obtained using the complete expression of the force in Eq. (2). This seems to indicate that small variations in the relative transverse beam sizes do not affect much the properties of the coherent modes.

For completeness, we consider here the case of head-on and long range collisions with alternating crossing when each bunch has two head-on collisions (one at each IP). Notice that now the incoherent tune shift is twice the beam-beam parameter. We also include the parasitic collisions *before* the IPs. The effective number of parasitic crossings per side of each IP is n_{par}. The kick is the same on both sides of the IP because the betatron phase advance of 180° compensates for the opposite direction of the beam-beam separation and therefore the long range collisions *before* and *after* the IP add up. We lump all the $2 \times n_{par}$ parasitic collisions in a a kick 90° after the IP. The spectrum of the motion of one bunch is illustrated in Fig. 11. We still have coherent modes outside the continuum, although the two modes with bigger tune shift seem to merge.

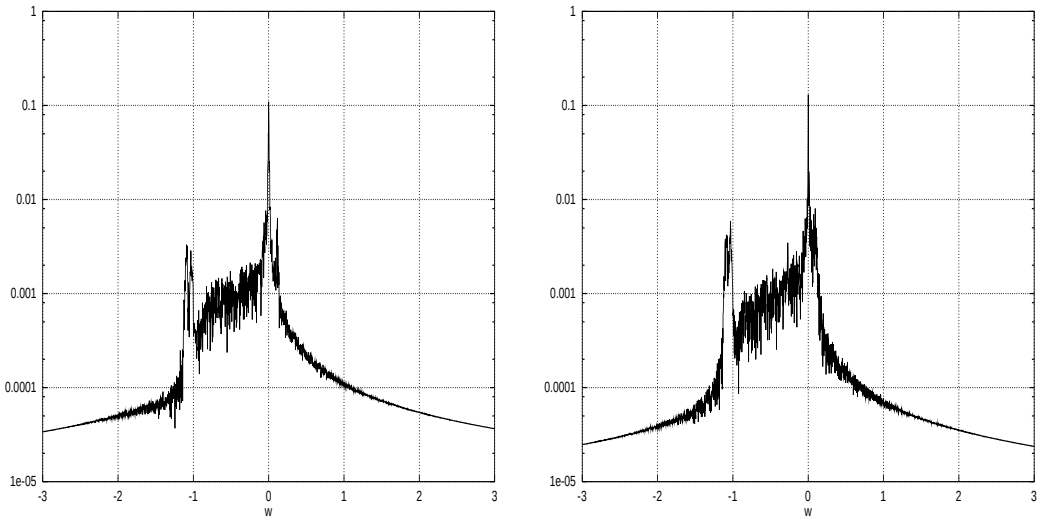

Figure 10: Spectrum in the case of head-on and long range collisions with alternating crossing (2^{17} turns, $N = 10^3$ macroparticles). Left: using the round beam approximation; right: using the complete expression for the force. The two planes of oscillation are equivalent and the coherent modes are shifted closer to the continuum. We still find 3 coherent modes outside the continuum which can not be Landau damped.

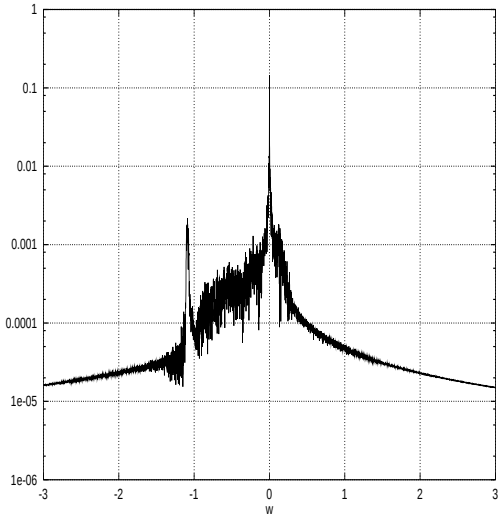

Figure 11: Spectrum in the case of head-on and long range collisions with alternating crossing (2^{17} turns, $N = 10^4$ macroparticles) when each bunch collides head-on at the two interaction points, and has long range collisions with $2 \times n_{par}$ bunches after each IP. The horizontal axis is in units of the new incoherent tune shift $2 \times \xi$: $w = \frac{\nu - Q}{2\xi}$.

6 Collision of bunches with unequal tunes

6.1 Head-on collisions

At the LHC-99 workshop, it was pointed out by A. Hofmann that the coherent frequency shifts can be reduced by separating the tunes of the two beams [6, 19]. The case of equal tunes for both beams is well known and leads to a σ-mode, with the beams oscillating in phase, and a π-mode, with an out of phase oscillation. In most storage rings the unperturbed betatron tunes are the same for both beams. But if the two unperturbed tunes can be made different, the beams are decoupled and oscillate on their own. In the LHC, with two independent rings, this could be easily realized.

We give an offset of ± 0.1 (in units of σ_x) to each beam in order to excite the oscillations for the head-on case with beam 1 at a tune $Q^{(1)} = 0.32$ and beam 2 at a tune $Q^{(2)} = 0.31$. Figure 12 shows that the continuum of beam 2 extends from $0.31 - \xi = 0.3066$ to 0.31. One of the two coupling modes is now inside the incoherent spread and Landau damping of this mode is restored. The continuum of beam 2 absorbs the energy of the lower-frequency coupling mode. At the same time, the amplitudes of the incoherent oscillation modes increase. The same will happen with beam 1 and its continuum, which extends from $(0.32 - \xi) = 0.3166$ to 0.32. Now we do not find any narrow peak corresponding to a coherent mode and we only observe a finite emittance growth.

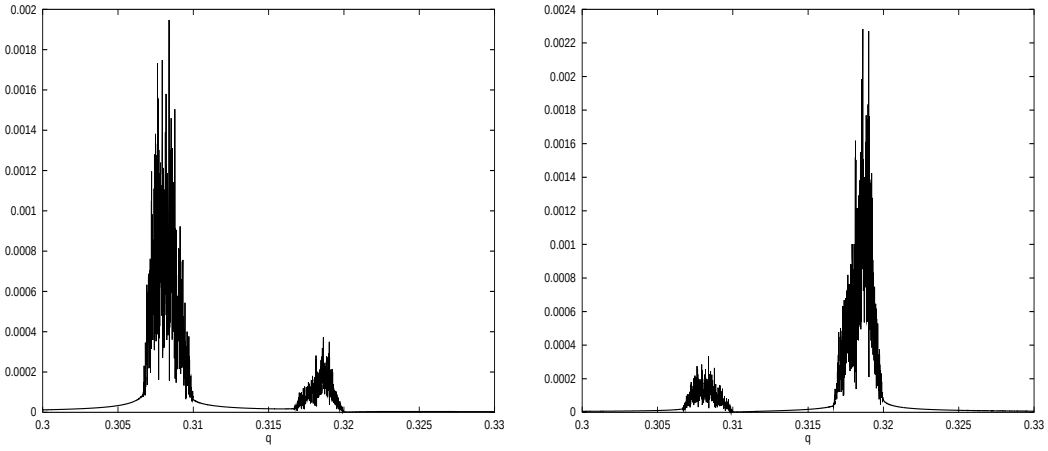

Figure 12: Beam 2 (left) and beam 1 (right) spectrum of centroid oscillation for head-on collisions with unequal tunes ($Q^{(1)} = 0.32$, $Q^{(2)} = 0.31$) and initial offset ± 0.1 (σ_x), (2^{17} turns, $N = 10^3$ macroparticles). Along the horizontal axis we plot the tune and along the vertical axis the corresponding amplitude. The new coupling modes are inside the continuum and are Landau damped.

The new frequencies of the coherent modes can be understood with a simple model. Two resonances determine the response of two beams with frequencies $Q^{(1)}$ and $Q^{(2)}$ to an external excitation. The frequencies of these resonances are [6, 19]

$$Q^2_{a,b} = \frac{(Q^{(1)})^2 + (Q^{(2)})^2}{2} + \frac{(-\xi)(Q^{(1)} + Q^{(2)})}{2} \pm \frac{1}{2}\sqrt{((Q^{(1)})^2 - (Q^{(2)})^2)^2 + 2(-\xi)(Q^{(1)} + Q^{(2)})(Q^{(1)} - Q^{(2)})^2 + (-\xi)^2(Q^{(1)} + Q^{(2)})^2}. \quad (17)$$

As the unperturbed tunes move apart, the tunes Q_a and Q_b of the two modes are more and more associated with the two individual beams respectively. If the tunes are very different

the beams are completely decoupled. For instance for $Q^{(1)} = 0.32$ and $Q^{(2)} = 0.31$ the new modes are at $Q_a = 0.3186$ and $Q_b = 0.3080$ (Q_a inside the continuum of beam 1 and Q_b inside the continuum of beam 2).

6.2 Long range collisions

We next consider the collision of 2 bunches with $Q^{(1)} = 0.32$ against 2 bunches with $Q^{(2)} = 0.31$, colliding head-on (no initial offset) at two IPs and including horizontal long range interactions in the same way as in Section 5.2. Again the horizontal and vertical spectra exhibit different tune shifts. As we have seen before, the head-on collisions give rise to coherent modes which lie in the continuum and are Landau damped. However, Fig. 13 (top), demonstrates that the long range collisions shift two of the coherent modes outside the continuum. Because the other two modes remain inside the continuum, they are Landau damped and not visible.

Choosing sufficiently different tunes for the two beams, for example $Q^{(1)} = 0.32$ (working point 1) and $Q^{(2)} = 0.24$ (working point 2), the two remaining coherent modes also merge with the continuum; see Fig. 13 (bottom).

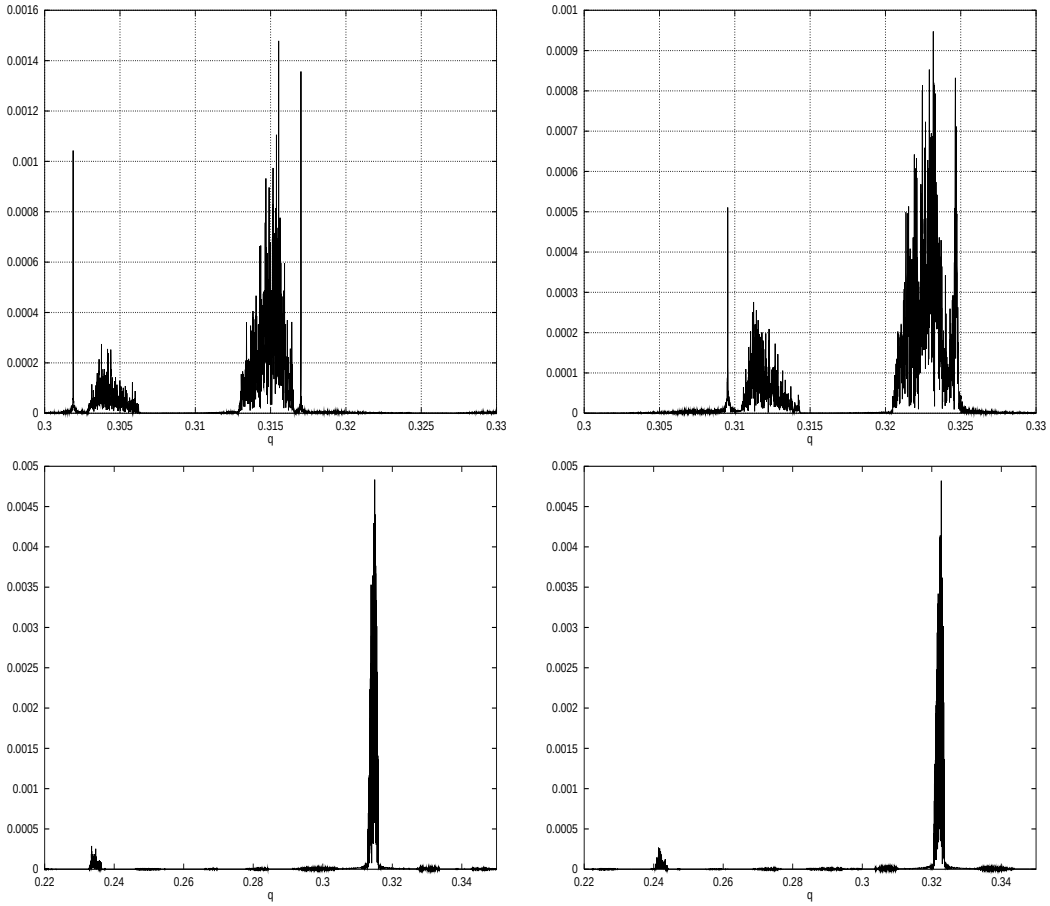

Figure 13: Spectrum of the vertical (left) and horizontal (right) motion of one of the bunches with $Q^{(1)} = 0.32$ with head-on collision and horizontal crossing (2^{17} turns, $N = 10^3$ macroparticles). Above, when the tune of beam 2 is $Q^{(2)} = 0.31$ the long range collisions shift two of the coherent modes outside the continuum. Below, when $Q^{(2)} = 0.24$ (working point 2) the tunes are sufficiently unequal and all the coherent modes merge the continuum and are Landau damped.

If we include alternating crossing, as in Section 5.3, even the coherent modes of the case $Q^{(1)} = 0.32$ and $Q^{(2)} = 0.31$ are brought back into the continuum and are Landau damped. In Fig. 14 we plot the spectrum of the bunch with $Q = 0.32$, for the case of alternating crossing.

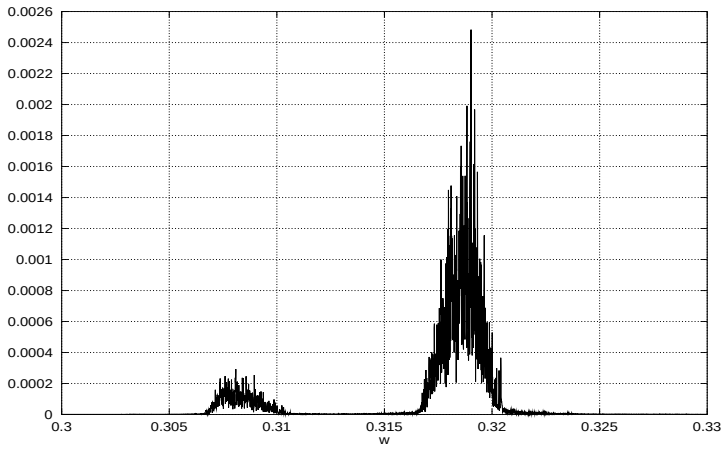

Figure 14: Spectrum of the centroid motion of one of the bunches with $Q^{(1)} = 0.32$ with head-on collision and alternating crossing when beam 2 has a tune $Q^{(2)} = 0.31$. Landau damping is restored for the 4 coherent modes.

7 Conclusions

Using a simplified multiparticle simulation, we have studied the coupled coherent beam-beam modes at the LHC.

For the case of head-on collisions and a finite initial transverse offset, the energy partition between the continuum, the σ- and the π-mode is found to be in agreement with theoretical predictions [1]. We have also confirmed another prediction [1] that, for a ratio of beam-beam parameters $0 < r \leq 0.6$, the π-mode lies within the continuum and that it is Landau damped. Its energy is transferred to the continuum, leading to an irreversible finite emittance growth. For equal beam-beam parameter of the two beams, we find a π-mode tune shift of -1.1 in units of ξ, sufficiently large to place it outside of the continuum and to lose Landau damping. We observe a decrease of the beam size with increasing fractional tune, which is explained by the dynamic beta effect. The tune shift of the π-mode is reduced as the fractional tune increases and, therefore, the π-mode moves closer to the continuum.

In the case of two equally strong beams with head-on and long range collisions, coherent modes exist outside of the continuum, even with alternating crossing at two IPs. In general, these modes are not Landau damped. However, if the betatron tunes of the two beams are sufficiently different, the frequencies of the coherent modes are shifted towards the continuum and Landau damping can be restored.

8 Acknowledgements

We thank W. Herr, E. Keil and F. Ruggiero for stimulating discussions and informations.

References

[1] Y.I. Alexahin, *On the Landau damping and decoherence of transverse dipole oscillations in colliding beams.* Particle Accelerators, Volume 59, p. 43 (April 1999).

[2] K. Yokoya, H. Koiso, *Tune shift of coherent beam-beam oscillations.* Particle Accelerators, 1990. Vol. 27, pp. 181-186.

[3] A. W. Chao, R. D. Ruth, *Coherent beam-beam instability in colliding beam storage rings.* SLAC/AP-37, 1984.

[4] I. Pool and F. Zimmermann (eds.), *Proceedings of the Workshop on Beam-Beam Effects in Large Hadron Colliders.* Geneva, April 12-17, 1999. CERN-SL-99-039 AP.

[5] A. Hofmann and O. Brüning, comments during the LHC-99 Beam-Beam Workshop.

[6] A. Hofmann, *Beam-beam modes for two beams with unequal tunes.* Proceedings of the LHC-99 Beam-beam workshop at CERN.

[7] M. Abramowitz and I.A. Stegun, *Handbook of Mathematical Functions.* Dover, New York, (1965) 297.

[8] E. Keil. *Nonlinear coherent effects between two strong bunched beams colliding in a storage ring.* Nuclear Instruments and Methods 188 (1981) 9-14.

[9] S. Matsumoto, K. Hirata, *A model of beam-beam interaction in e^+e^- storage rings with dipole and quadrupole modes.* KEK preprint 92-146. November 1992. A.

[10] W. Herr. *Coherent dipole oscillations and orbit effects induced by long range beam-beam interactions in the LHC.* CERN-SL/91-34 (AP) and LHC Note 165.

[11] E. Keil, *Visible frequencies in the nonlinear coherent beam-beam effect.* CERN-LEP-NOTE-294, Apr 1981.

[12] A.W. Chao, *Physics of Collective Beam Instabilities in High Energy Accelerators.* John Wiley & Sons. 1993.

[13] J. Gareyte, *Beam-beam design criteria for LHC.* Proceedings of the Beam-beam-99 workshop at CERN.

[14] A. Chao, *Coherent beam-beam effects.* SSCL-346. January 1991.

[15] A. Hofmann, S. Myers, *Evaluation of the Absolute LEP Luminosity from Measurement of the Coherent Beam-Beam Tune Split.* LEP Note 604. 1988.

[16] D. Cinabro et al., *Observation of the Dynamic Beta Effect at CESR with CLEO.* CLNS 97/1496. CLEO CONF 97-11. EPS Abstract 356 (1998).

[17] D. Brandt, W. Herr, M. Meddahi, A. Verdier. *Is LEP beam-beam limited at its highest energy?.* PAC Proceedings, New York, pp. 3005-3007, 1999.

[18] W. Herr, *Tune Shifts and Spreads due to Short and Long Range Beam-Beam Interactions in the LHC*, CERN SL/90-06 (AP) (1990).

[19] The SPEAR Group: R.H. Helm, M.J. Lee, M. Matera, P.L. Morton, J.M Paterson, B. Richter, A.P. Sabersky, H. Wiedemann, P.B. Wilson, M.A. Allen, A.E. Augustin, G.E. Fischer, *Beam-Beam Coupling in SPEAR*, Proc. IX Int. Conf. High Energy Accelerators, SLAC, page 66.